Characterization of $In_xGa_{1-x}As$ Tunnel Junction Light-Emitting Transistors

Cheng-Han Wu and Chao-Hsin Wu
Graduate Institute of Photonics and Optoelectronics, National Taiwan University,
No. 1, Sec. 4, Roosevelt Road, Taipei, 10617 Taiwan (R.O.C)
Email: chaohsinwu@ntu.edu.tw
Phone: +886-2-3366-3694

Keywords: Light emitting transistor, tunnel junction

Abstract

We report the electrical and optical characteristics of tunnel junction light-emitting transistors (TJLETs) with varying the indium mole fraction (x= 5% and 2.5%) of the $In_xGa_{(1-x)}As$ base-collector tunnel junctions. The smaller band gap energy due to higher indium composition leads to stronger Franz-Keldysh absorption and direct tunneling probability when BC junction is reverse-biased, which results in the larger current gain growth and the less optical output enhancement.

INTRODUCTION

The III-V light-emitting transistors (LETs) function as three-port devices (an electrical input, an electrical output, and a "third-port" optical output) by incorporating quantum wells (QWs) in the base layer of heterojunction bipolar transistior (HBT) to enhance the radiative recombination [1][2]. If the base region is afforded adequate *Q*, the laser operation of the LET can be achieved, namely, the transistor laser (TL) [3]-[5]. As shown elsewhere [6], the recombination optical signal, via internal Franz-Keldysh (F-K) absorption [7], causes voltage-dependent breakdown and negative resistance in the TL collector characteristics [8]. Moreover, the high doping p^+ and n^+ tunnel junction (TJ) has been employed at the base-collector (BC) junction to enable the laser operation to be more effectively controlled by changes of voltages, which makes possible a direct voltage modulation laser along with an usual current modulation operation [9][10]. It is possible to realize voltage-operated switching and use it also in signal-mixing and data processing [6]. In the present work we investigate the effect of different indium mole fraction of the $In_xGa_{(1-x)}As$/AlGaAs tunnel junction light-emitting transistor (TJLET). The smaller band gap energy due to higher indium composition leads to stronger F-K absorption and direct tunneling probability under applied reverse BC voltage. This effect contributes to the higher current gain growth and the less optical output enhancement.

DEVICE FABRICATION

The crystal epitaxial layers in the present work consists (from the GaAs substrate upward) of a 2000 Å *n*-type heavily doped GaAs buffer layer, followed by a 3300 Å *n*-type contact layer, a graded $Al_{0.4}Ga_{0.6}As$ to $Al_{0.8}Ga_{0.2}As$ oxide buffer layer, a 4000 Å *n*-type $Al_{0.95}Ga_{0.05}As$ oxidizable layer, and then a graded $Al_{0.8}Ga_{0.2}As$ to $Al_{0.4}Ga_{0.6}As$ oxide buffer layer that forms the bottom cladding layers. These layers are followed by a 250 Å *n*-type GaAs, a 150 Å *n*-type $In_xGa_{(1-x)}As$ (x=5% and 2.5%) and a 300 Å *p*-type $Al_{0.1}Ga_{0.9}As$ that completes the tunnel junction. The base layer includes a 1100 Å *p*-type GaAs with an undoped (120 Å for x=5% and 150 Å for x=2.5%) $In_{0.2}Ga_{0.8}As$ QW (designed for $\lambda \approx$ 980nm). Finally, the epitaxial TJLET structure is completed with a 250 Å *n*-type $In_{0.49}Ga_{0.51}P$ wide-gap emitter layer, the upper cladding layers (the same as the bottom ones), and a 1000 Å heavily doped *n*-type contact layer. The schematics of device structure and layout are shown in Fig. 1.

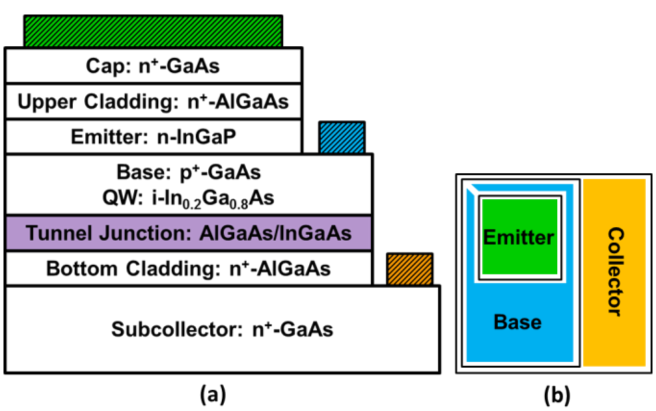

Fig. 1: Schematic of the device (a) cross section and (b) top view of TJLET. The emitter metal size is 60×60μm^2.

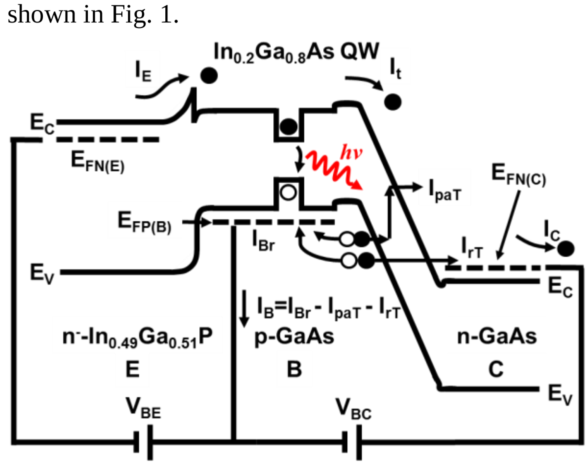

Fig. 2: Schematic band diagram of the tunnel junction light-emitting transistors operate in forward active mode.

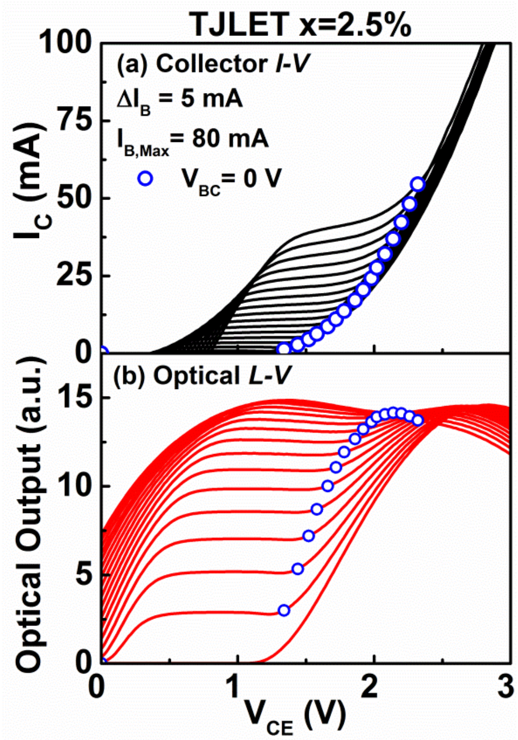

Fig. 3: (a) The collector *I-V* characteristics of an emitter-metal-size 60×60μm^2 TJLET (for $In_xGa_{(1-x)}As$ tunnel junction x=2.5%) showing the negative resistance phenomenon (V_{CE}≈1V) and tunneling effect (V_{CE}>2V). (b) The optical *L-V* characteristics shows holes resupply back to QW to enhance the optical output (V_{BC}<0V). The light intensity become saturation and decreasing via F-K absorption under stronger reverse-biased BC junction field.

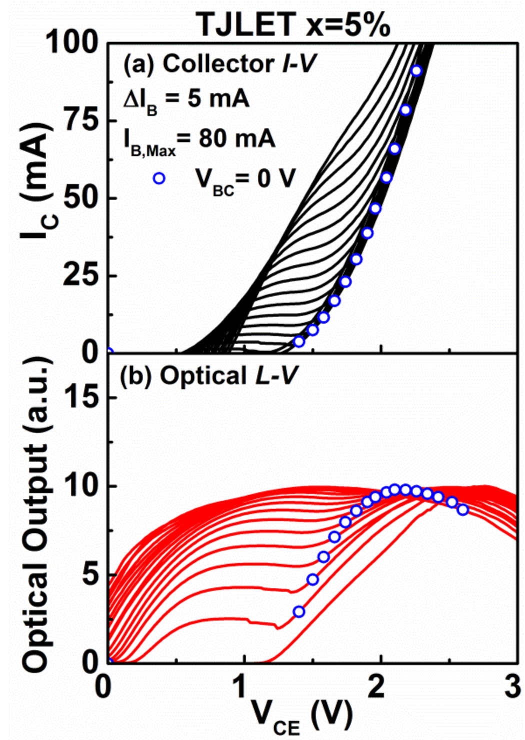

Fig. 4: (a) The collector *I-V* characteristics and (b) Optical *L-V* characteristics of an emitter-metal-size 60×60μm^2 TJLET (for $In_xGa_{(1-x)}As$ tunnel junction x=5%).

The devices are fabricated using standard optical lithography and chemical wet etching. We use the dilute sulfuric acid to form the emitter mesa. A dilute hydrochloric acid solution is used as selective etch for InGaP between emitter and base layers. The base and isolation mesas are also formed by the same method. A Ti/Pt/Au metal is deposited as *p*-type base contact after emitter mesa etching is completed. An Au-Ge/Ni/Au metal is applied for the emitter and collector ohmic contact. We use polyimide as the passivation step, followed by a via-hole step and one metal interconnection step to finish the devices.

CURRENT COMPONENTS

Figure 2 shows the schematic band diagram of the TJLET operating in forward-active mode. Electrons injected from the emitter into the base region are captured by the InGaAs QW and recombine radiatively with supply of holes via usual base ohmic contact. The minority carriers of injected electrons that do not recombine in the base will be swept to the collector as transport current (I_t). At high reverse bias of base-collector junction, photons can be absorbed and create additional electron-hole pairs via F-K photon-assisted tunneling. It leads to additional current (I_{paT}) to collector current (I_C), and resupplies holes back to base region. I_{rt} represents the current contributes to collector current (I_C) by band-to-band direct tunneling from tunnel junction. The collector current (I_C) shown in Eq. (1) can be thus expressed as the sum of conventional transport current (I_t), photon-assisted tunneling portion (I_{paT}), and direct tunneling current (I_{rT}). The base recombination current (I_{Br}) consists of the base current provided from ohmic contact (I_B), the resupplied holes from photon-assisted tunneling (I_{paT}), and direct tunneling current from tunnel junction (I_{rT}), as shown in Eq. (2)

$$I_C = I_t + I_{rT} + I_{paT} \tag{1}$$

$$I_{Br} = I_B + I_{rT} + I_{paT} \tag{2}$$

RESULT AND DISCUSSION

Figure 3 shows (a) the collector *I-V* and (b) optical *L-V* characteristics of the emitter-metal-size of 60×60μm^2 TJLET with the base current (I_B) varying from 0 to 80 mA. The indium mole fraction of the $In_xGa_{(1-x)}As$ tunnel junction is 2.5%. The blue circles are the points where V_{BC} equals to zero. When V_{CE} ≈ 1V, the BC tunnel junction is operated in the negative resistance region, leading to an alleviated or even descendant trend in the *I-V* curve. The upward slope in the collector current, I_C versus V_{CE}, is the evident of tunneling effects. I_C increases as the function of V_{CE} owing to F-K (photon-assisted) absorption and direct tunneling (non photon-assisted) ($I_C = I_t + I_{paT} + I_{rT}$).

The optical *L-V* characteristic is shown in Fig. 3(b). Reverse-biased BC junction supply more holes to the quantum well active region, resulting in additional optical output enhancement. However, under stronger reverse-biased BC junction field (V_{CE}>2.5V), optical output is reduced by F-K absorption.

Figure 4 shows the other TJLET with 5% indium content at its tunnel junction. Compared with the previous sample (x = 2.5%), the optical output of this one (x=5%) is smaller due to the narrower QW (150 Å to 120 Å). Correspondingly, the electrical current gain is larger because fewer carriers are captured by the QW and therefore more contribute into transport current (I_t). However, the tunneling process occurs predominantly when BC junction turns into reverse-biased. The influence of QW on electrical and optical characteristics becomes minor afterward. Furthermore, the directly tunneling probability can be obtained by using the Wentzel-Kramers-Brillouin (WKB) approximation [11]. The tunneling probability is shown in Eq. (3). The more indium content at the $In_xGa_{(1-x)}As$ tunnel junction, the smaller band gap energy and leads to the greater tunneling probability. The tunneling probability is 2.64×10^{-12} for x = 2.5% and 4.21×10^{-12} for x = 5%.

$$P_t \cong \exp\left[-2\int_{x_1}^{x_2}\sqrt{2m^*(E_c - E_f)/\hbar^2}\,dx\right] \qquad (3)$$

The other tunneling effect is band-to-band F-K absorption [7]. With electrical field applied and photon absorption presented, the barrier height is reduced to $E_g - \hbar\omega$ and electrons will be easier to tunnel through the barrier. For x = 5% tunnel junction, the smaller band gap energy leads to more photons absorption and more electron-hole pair generation. The electroabsorption coefficient is given by

$$\alpha(\hbar\omega, E) = 1.0\times10^4\,(f/n)(2m_r/m)^{4/3}E^{1/3}\int_{\beta}^{\infty}|Ai(z)|^2\,dz \qquad (4)$$

$$\beta = 1.1\times10^5(2m_r/m)^{1/3}(E_g - \hbar\omega)/(E^{2/3}) \qquad (5)$$

Figure 5 shows the electrical current gain and optical output when BC junctions are under eight different reverse-biased junction field with I_B=40mA. The higher current gain growth and the less optical output enhancement for indium content x = 5% TJLET results from its smaller band gap energy, stronger F-K absorption, and direct tunneling probability. The optical output reduction under stronger reverse-biased BC junction field is on account of the stronger F-K absorption.

Conclusions

In conclusion, we have demonstrated that the higher the indium content at the $In_xGa_{(1-x)}As$ tunnel junction of TJLET, the smaller band gap energy leads to stronger F-K absorption and direct tunneling probability when BC junction is reverse-biased. This results in the higher current gain growth and the less optical output enhancement. Moreover, tunnel junction enables a direct voltage-controlled modulation via photon-assisted (F-K) tunneling. This is an advantage in microwave modulation and signal-mixing.

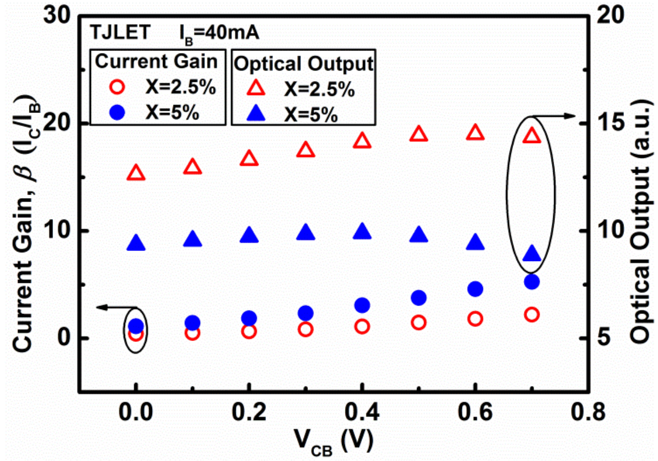

Fig. 5: The electrical current gain and optical output when BC junctions are under eight different reverse-biased junction field and I_B=40mA.

References

[1] M. Feng, N. Holonyak, Jr., and W. Hafez, Appl. Phys. Lett. 84, 151 (2004).

[2] M. Feng, N. Holonyak, Jr., and R. Chan, Appl. Phys. Lett. 84, 1952 (2004).

[3] G. Walter, N. Holonyak, Jr., M. Feng, and R. Chan, Appl. Phys. Lett. 85, 4768 (2004).

[4] R. Chan, M. Feng, N. Holonyak, Jr., and G. Walter, Appl. Phys. Lett. 86, 131114 (2005).

[5] M. Feng, N. Holonyak, Jr., G. Walter, and R. Chan, Appl. Phys. Lett. 87, 131103 (2005).

[6] A. James, N. Holonyak, Jr., M. Feng, and G. Walter, IEEE Photonics Technol. Lett. 19, 680 (2007)

[7] C. M. Wolfe, N. Holonyak, Jr., and G. E. Stillman, *Physical Properties of Semiconductors* (Prentice Hall, Englewood Cliffs, NJ, 1989), pp. 219-220.

[8] A. James, G. Walter, M. Feng, and N. Holonyak, Jr., Appl. Phys. Lett. 90, 152109 (2007).

[9] M. Feng, N. Holonyak, Jr., H. W. Then, C.H. Wu, and G. Walter, Appl. Phys. Lett. 94, 041118 (2009).

[10] M. K. Wu, M. Feng, and N. Holonyak, Jr., Appl. Phys. Lett. 101, 081102 (2012).

[11] D. E. Mars, Y.-L. Chang, M. H. Leary, and S. D. Roh, Appl. Phys. Lett. 84, 2560 (2004).

Acronyms

LET: Light-Emitting Transistor
TJLET: Tunnel Junction Light-Emitting Transistor
QW: quantum well
HBT: heterojunction bipolar transistior
TL: transistor laser
BC: base-collector
F-K: Franz-Keldysh
WKB: Wentzel-Kramers-Brillouin